Surviving Wi-Fi Interference in Low Power ZigBee Networks

Chieh-Jan Mike Liang[†], Nissanka Bodhi Priyantha[‡], Jie Liu[‡], Andreas Terzis[†]

[†]Department of Computer Science
Johns Hopkins University
Baltimore, MD

[‡]Microsoft Research
One Microsoft Way
Redmond, WA

{cliang4, terzis}@cs.jhu.edu {jie.liu, bodhip}@microsoft.com

Abstract

Frequency overlap across wireless networks with different radio technologies can cause severe interference and reduce communication reliability. The circumstances are particularly unfavorable for ZigBee networks that share the 2.4 GHz ISM band with WiFi senders capable of 10 to 100 times higher transmission power. Our work first examines the interference patterns between ZigBee and WiFi networks at the bit-level granularity. Under certain conditions, ZigBee activities can trigger a nearby WiFi transmitter to back off, in which case the header is often the only part of the Zig-Bee packet being corrupted. We call this the symmetric interference regions, in comparison to the asymmetric regions where the ZigBee signal is too weak to be detected by WiFi senders, but WiFi activity can uniformly corrupt any bit in a ZigBee packet. With these observations, we design *BuzzBuzz* to mitigate WiFi interference through header and payload redundancy. *Multi-Headers* provides header redundancy giving ZigBee nodes multiple opportunities to detect incoming packets. Then, *TinyRS*, a full-featured Reed Solomon library for resource-constrained devices, helps decoding polluted packet payload. On a medium-sized testbed, BuzzBuzz improves the ZigBee network delivery rate by 70%. Furthermore, BuzzBuzz reduces ZigBee retransmissions by a factor of three, which increases the WiFi throughput by 10%.

Categories and Subject Descriptors

C.2.1 [**Computer-Communications Networks**]: Wireless Communication

General Terms

Design, Experimentation, Measurement, Performance

Keywords

802.11 Interference Mitigation, 802.15.4, Wireless Measurement Study, Error Correction

1 Introduction

We have witnessed over the last ten years a proliferation of wireless technologies that have now become ubiquitous. Given the scarce availability of RF spectrum, many of these technologies are forced to use the same unlicensed frequency bands. For example, IEEE 802.11 (WiFi), IEEE 802.15.1 (Bluetooth) and IEEE 802.15.4 (ZigBee)[1] all share the same 2.4 GHz ISM band. *Cross Technology Interference (CTI)* is a consequence of this coexistence that can lead to loss of reliability and inefficient use of the radio spectrum.

The majority of MAC protocols are designed to share the communication medium among nodes that understand the same PHY layer. In this model CTI is considered the same as random background noise, despite the fact that it can cause significant performance degradation. Even worse, system designers have little means to coordinate across networks that use different wireless standards since they usually belong to different administrative domains. CTI is especially unfavorable for 802.15.4-based wireless sensor networks that have to counter the effects of severe interference from ubiquitous 802.11 deployments.

We motivate the problem that CTI causes to sensors networks using our experience from a sensor network deployment. In this deployment, we placed a network of 90 Genomote motes [16] within a 140,000 square feet lecture hall. The motes ran a building energy management application and used four 15.4 channels simultaneously. 16 Xirrus XN8 WiFi arrays were deployed in the same space. Each WiFi array integrates eight access points, which collectively use all WiFi channels across the entire space. During the Microsoft PDC conference in 2008, 7,000+ people sat in the lecture hall and at the peak time, more than 2,500 people were connected to the WiFi network. Figure 1 shows the number of nodes from the sensor network deployment that successfully reported data over an ten hour period. The WiFi activity during the first four hours completely stressed the

---

[1]Technically, the IEEE standards and industrial alliances are different. Since this paper primarily considers the PHY and MAC layer interactions among these wireless networks, we make no distinction between WiFi and IEEE 802.11, likewise between ZigBee and IEEE 802.15.4. Furthermore, to shorten the presentation, in the rest of this paper, we will use the terms 802.15.4 and 15.4 interchangeably. We will also invoke the names of the standard's different variants (i.e., 802.11b/g) whenever necessary.
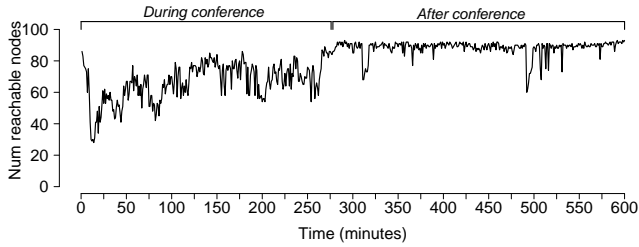
Figure 1. The number of sensor nodes reporting data over ten hours. Thousands of users were connected to a co-located WiFi network during the first four hours causing dramatic interference to the sensor network.
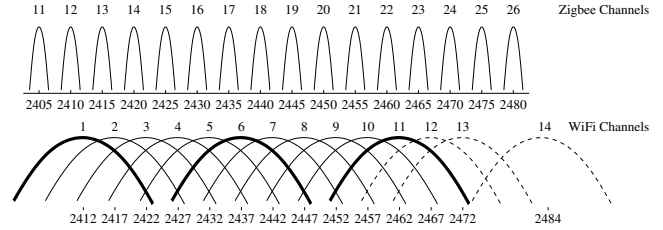

Figure 2. 802.11b/g and 802.15.4 frequency channels in the 2.4 GHz ISM band. Each 802.11 channel is 22 MHz wide, while 802.15.4 channels are 2 MHz wide.

radio bands and left more than half of the sensor nodes unreachable.

This result is supported by multiple previous studies that have shown that 15.4 performance significantly degrades in the presence of 802.11 interference [6, 18, 25, 28]. The unanimous pessimistic conclusion of those studies was that the only way to mitigate such interference is for the 15.4 network to *avoid* the channels occupied by 802.11.

There are two ways to pursue interference avoidance: *static channel assignment* and *dynamic channel assignment (i.e., channel hopping)*. In a static channel assignment scheme, one assumes that the 802.11 network occupies a fixed number of channels and the 15.4 network is provisioned to use frequency bands that are left unused by WiFi. As Figure 2 suggests, this assignment leaves at most two 15.4 channels free from potential 802.11 interference. Furthermore, static channel assignment may not work as planned due to node mobility [6] and incremental WiFi deployments.

In dynamic channel assignment schemes, different nodes in a sensor network, or the same node over different points in time, will use different 15.4 channels to avoid interference from nearby WiFi sources. These mechanisms face two challenges: detect the presence of 802.11 traffic [6, 18] and coordinate channel selection among 15.4 senders and receivers [28]. In addition to the coordination complexity, interference avoidance mechanisms leave large portions of the spectrum unused even when there is little 802.11 traffic in them. This inefficiency is especially damaging for large and dense sensor networks that cannot support the desired application throughput using a single 15.4 channel [16, 30].

Instead of trying to avoid interference from 802.11 traffic, the goal of this paper is to improve the coexistence of 15.4 and 802.11 networks that operate in the overlapping frequency channels. Our approach is based on insights derived from a thorough examination of the interactions between the two radio technologies. In particular, we make several key observations that previous work has overlooked: **(1)** In the time domain, 802.11 packets are typically much shorter than 15.4 packets, so they cause bursty bit errors in 15.4 packets. **(2)** A large percentage of dropped 15.4 packets are due to corruptions in the packet headers, especially when the 15.4 transmitter is close to an 802.11 transmitter. **(3)** We experimentally found that when a 15.4 node is close to an 802.11 transmitter, a 15.4 packet can actually cause the 802.11 transmitter to back off, due to elevated channel energy. When this

happens, 802.11 *only* corrupts the 15.4 packet header (which causes frequent packet losses), but the remainder of the 15.4 packet is left unaffected.

Depending on how 802.11 and 802.15.4 transmitters interact, we partition the interfere domain of the two radios into *symmetric* and *asymmetric* regions. In symmetric regions, a 15.4 transmission can cause nearby 802.11 transmitters to back off, so the receiving bit corruption happens mainly in 15.4 packet headers. We employ a simple yet effective header redundancy mechanism, called Multiple-Headers (MH), to address this packet header corruption problem. MH sends the header multiple times in a single 15.4 packet. The first (corrupted) header will cause the 802.11 transmitter to back off, ensuring that the second header can be correctly detected by the 15.4 receiver. In asymmetric regions, the 15.4 signal is too weak to affect 802.11 behavior. In this case, we use a forward error correction (FEC) code to correct bit errors that occur across the entire 15.4 packet. We examine Hamming and Reed-Solomon (RS) codes and find that RS code is particularly effective against the bursty error patterns we observed.

We integrate these techniques into the *BuzzBuzz* protocol. BuzzBuzz resides at the MAC layer and provides a general-purpose, single hop reliable delivery mechanism that can counter the effects of 802.11 interference. We implemented BuzzBuzz in TinyOS and evaluated its performance on a 57-node testbed under heavy WiFi interference. Specifically, we compare the performance of the Collection Tree Protocol (CTP) [3] with and without BuzzBuzz. The results show that BuzzBuzz improves the packet delivery ratio by 70% and reduces the number of packet retransmissions by a factor of three. Reducing the number of packet re-transmissions from the sensor network leads to less interference to the WiFi network and ultimately higher throughput for 802.11 as well. Thus, BuzzBuzz creates a win-win situation in a crowded spectrum space.

The paper makes the following *contributions*: **(1)** We are the first to examine and quantify the interference patterns between 802.11 and 802.15.4 networks *at a bit-level granularity*. **(2)** We explain how a 802.15.4 node may change the behavior of nearby 802.11 transmitters creating symmetric interference between the two radios. Based on these observations, we introduce targeted redundancy mechanisms, namely MH and FEC, that improve 15.4 reception rate. **(3)** We present a complete implementation of a Reed-Solomon (RS) library suitable for resource-constrained motes. **(4)**
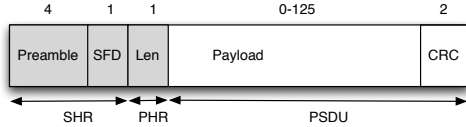
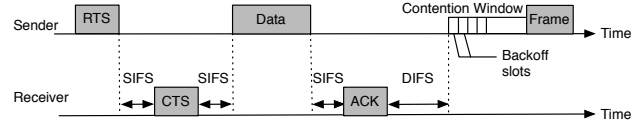**Figure 3. Format of a 15.4 packet. Field sizes are in bytes.**

Figure 4. Messages and delays defined in the 802.11 MAC protocol. Durations of packet transmissions and time intervals depend on the 802.11 variant used. The leading RTS/CTS exchange is used only for large packets.

We evaluate a TinyOS implementation of BuzzBuzz through stress tests in a testbed.

The rest of the paper is organized as follows. We provide a brief overview of the WiFi and ZigBee protocols in Section 2 where we also illustrate the potential for interference between the two radio technologies. Section 3 presents the methodology we used to quantify the interactions between co-located 802.11 and 15.4 networks and an in-depth analysis of the root causes for the observed packet losses. In Section 4 we present techniques for protecting 15.4 packets from 802.11 senders located in the symmetric and asymmetric regions, while in Section 5 we describe BuzzBuzz and evaluate its performance on a 57-node TelosB testbed. We present related work in Section 7 and conclude in Section 8.

2 Background

In order to mitigate the impact of cross-technology interference and improve the performance of 802.15.4 networks under 802.11 interference, we need to delve into the details of how these radio technologies interact. We summarize their salient features in the rest of this section.

2.1 802.15.4 Overview

The IEEE 802.15.4 standard defines a PHY layer for low-rate wireless networks operating in the 2.4 GHz ISM band [9]. The standard defines 16 channels within this band, each 2 MHz wide with 3 MHz inter-channel gap-bands (see Figure 2). According to the standard, outgoing bytes are divided into two 4-bit *symbols* and each symbol is mapped to one of 16 pseudo-random, 32-chip sequences. The radio encodes these chip sequences using orthogonal quadrature phase shift keying (O-QPSK) and transmits them at 2 Mchips/s (i.e., 250 kbps).

Figure 3 shows the format of a 15.4 packet including the Synchronization Header (SHR) and the PHY Header (PHR), shown in grey. The SHR header includes a 4-byte preamble sequence (all bytes set to `0x00`) and a 1-byte Start of Frame Delimiter (SFD) set to `0x7A`. The PHR includes a 1-byte Length field that describes the number of bytes in the packet's payload, including the 2-byte CRC. The maximum packet size is 133 bytes, including all the headers.

The MAC protocol in the 802.15.4 standard defines both beacon-enabled and non-beacon modes. In the beaconless mode, the standard specifies using a CSMA/CA protocol [9]. While the CSMA/CA protocol uses binary exponential backoff, in practice the CSMA/CA protocol implemented in TinyOS uses a fixed-length backoff interval [29].

On the receiving side, a 15.4 radio synchronizes to incoming zero-symbols and searches for the SFD sequence to receive incoming packets. Interference and noise can corrupt the incoming chip stream, leading to 32-chip sequences that do not match one of the 16 valid sequences. The receiver

then maps the input sequence to the valid sequence with the smallest Hamming distance.

We note that some 802.15.4 radios (e.g., CC2420 [26]) provide a user-defined *correlation threshold* that controls the maximum Hamming distance between the received 32-chip sequence and the valid SFD sequence that the receiver is willing to tolerate. If this threshold is high, the received signal must closely match the ideal signal, hence the signal-to-noise ratio should be high. If this threshold is low, the receiver allows a low signal-to-noise ratio at the expense of potentially interpreting corrupted packets or channel noise as valid packets.

2.2 802.11 Overview

WiFi networks are almost ubiquitous in office buildings, homes, and even outdoors in urban areas. Considering that 802.11b, 802.11g, and 802.11n share the same 2.4 GHz ISM band with 802.15.4, 802.11 transmissions can interfere with co-located 802.15.4 networks. In the U.S., only 15.4 channels 25 and 26 do not overlap with WiFi and even these channels are covered in other parts of the world. In practice, since most WiFi networks use channels 1, 6, and 11, 15.4 channels 15 and 20 can also be interference-free [16]. The potential for 802.11 transmissions to overwhelm 15.4 receivers is amplified by the fact that 802.11 radios transmit at 10 to 100 times higher power than 15.4 radios.

Figure 4, which presents the key features of the 802.11 MAC protocol through a timing diagram, helps us understand how WiFi nodes use the wireless medium. The 802.11 standard specifies using CSMA/CA with ACKs as the MAC protocol, optionally with the addition of RTS/CTS packets [10]. The protocol also specifies the SIFS and DIFS intervals when nodes should defer using the medium.

A time period, called the contention window, follows the DIFS shown in Figure 4. This window is divided into slots. Nodes use a uniform random distribution to select a slot and wait for that slot before attempting to access the medium. The node that selects the earliest slot wins while others defer. Nodes initialize their contention window (CW) to 31 slots and double it every time they fail to access the medium, until CW reaches a maximum size of 1023 slots.

Table 1 summarizes the duration of the DIFS, SIFS, and backoff slots for 802.11b and 802.11g. Also shown are the maximum and minimum packet sizes for 802.11b, 802.11g, and 802.15.4. It is worth noting that for many 802.11b and 802.11g packets, the entire air time is smaller than a 802.15.4 slot time. Based on the relatively small time intervals between 802.11 transmissions, one can easily see that a backlogged 802.11 sender can potentially corrupt the vast ma-

Parameter	802.15.4	802.11b	802.11g
SIFS	N/A	30 μs	10 μs
DIFS	N/A	50 μs	28 μs
Slot time	320 μs	20 μs	9 μs
Initial CW	1-32	0-31	0-31
Successive CWs	1-8	BEB	BEB
Min length packet	352 μs	202 μs	194 μs
Max length packet	4,256 μs	1,906 μs	542 μs

Table 1. Packet and interval durations for 802.11 and 802.15.4. The length of the contention windows (CW) for 802.15.4 corresponds to the MAC used by TinyOS. The 802.11 standard uses Binary Exponential Backoff (BEB).

jority of 802.15.4 packets. In the section that follows we experimentally measure the extent of this interference.

3 Measuring WiFi and Zigbee Interactions

We conduct a series of experiments that proceed from quantifying the macroscopic impact of 802.11 interference to 15.4 networks, to exposing the low-level interactions between the two networks that generate the high-level behaviors we observe. The knowledge of when and how 15.4 packets are corrupted is used to develop a set of compensation techniques that markedly improve the coexistence between the two radio technologies.

3.1 Methodology

Most of the previous work that has examined the interaction between 802.11 and 802.15.4 networks has focused on high-level metrics such as packet reception rate (PRR) [4, 23]. In contrast, we examine the interaction between the two radio technologies by accurately detecting and measuring various packet transmission events. Given the packet and interval durations shown in Table 1, this task requires instruments that detect and measure RF events that are as short as a few μs.

The RFMD ML2724 narrow band radio gives us the ability to detect RF transmissions with the desired timing accuracy and precision [22]. The ML2724 can be tuned to a central frequency between 2400 and 2485 MHz and generates an analog voltage on its RSSI_OUT pin that is directly proportional to the RF signal energy received in a 2 MHz frequency band centered at the tuned frequency. Given the relative widths of the channels used by 802.11, 15.4, and the ML2724 radio, it is possible to detect 802.11 packets that collide with 15.4 transmissions without being affected by the later transmissions. In practice, we use 15.4 channel 22, 802.11 channel 11, and set the ML2724's center frequency to 2465.792 MHz (equivalent of 15.4 channel 23).

We selected the ML2724 for two key reasons. First, RSSI measurements are directly available as analog voltage outputs, which makes it possible to detect RSSI changes quickly by sampling this signal at a high frequency. In contrast, the CC2420 radio exposes the measured RSSI value as the contents of an internal register; due to the delays associated with accessing CC2420 registers over the SPI bus, it is impossible to detect most of the 802.11 RF events by reading this RSSI register. The second reason for using the ML2724 is its fast RSSI response. According to the datasheet, the maximum rise and fall times of the RSSI_OUT are 4.5 μs and 3 μs respectively, which make ML2724 an excellent candidate for

detecting the RF activity we are interested in.

While we use the ML2724 radio to detect 802.11 packets, we detect events related to the transmission of 15.4 packets using the GPIO pins of TelosB motes equipped with CC2420 radios [20]. Specifically, we leverage the observation that the TinyOS event, CaptureSFD.captured is invoked at the beginning and the end of 15.4 packet transmissions respectively. This event is the interrupt service handler that is triggered when the CC2420 radio toggles its pin at specific points during a radio packet transmission. Under light load, when interrupts are disabled only for short durations, we can accurately detect these CC2420 events by toggling processor GPIO pins from within these TinyOS events. There is however a fixed offset between the actual RF transmissions and the toggling of pins on the CC2420 radio. We measured these offsets by observing the RSSI_OUT of a properly tuned ML2724 and the GPIO pin activities of a TelosB mote using an oscilloscope; during these measurements, we also verified that these offsets are constant.

To accurately correlate 802.11 and 802.15.4 transmissions over time we connected the RSSI_OUT pin of the ML2724 radio and the mote's GPIO pins to the same Data Acquisition (DAQ) card that samples and logs analog inputs at 1 MHz frequency [17].

3.2 802.15.4 Packet Reception Ratio

The goal of the first experiments is to quantify at a high level the impact of 802.11 interference on 15.4 links. Considering that lost 15.4 frames must be retransmitted at the cost of increased latency and energy consumption, we adopt packet reception ratio (PRR) as the pertinent metric for this experiment.

Experiment setup. Indoor environments are most likely to house overlapping 802.11 and 15.4 networks and for this reason we performed a controlled experiment in the basement of a parking garage. The parking garage had minimal structural obstructions, enabling us to examine the interference under a wide range of inter-node distances. The basement also minimized the external RF interference on our experiments; a Wi-Spy spectrum analyzer verified that there was very low interference from other RF sources.

The 802.11 network in this experiment consists of an 802.11 b/g access point and a laptop equipped with an 802.11 wireless radio configured in infrastructure mode. This laptop generates a stream of 1,500-byte TCP segments using the iperf tool. To measure the worst-case impact on the 15.4 network, we configure iperf to transmit as quickly as possible. Another laptop, connected to the access point through an Ethernet cable, acts as the traffic sink for the WiFi network. To ensure that our results are not biased by the implementation details of a specific 802.11 chipset, we repeat the experiment using multiple access points manufactured by Belkin, Linksys, and Netgear, with Broadcom or Atheros chipsets. All access points produced similar results.

The 802.15.4 network consists of TelosB motes equipped with 802.15.4-compliant TI CC24240 radios [26] running TinyOS 2.1. A dedicated sender sends one max-size packet (i.e., 128 bytes of payload) every 75 ms. These parameters correspond to the sending rate of a high data-rate WSN ap-
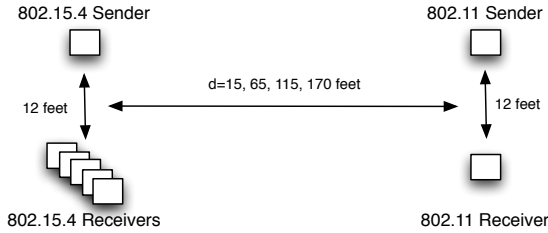
Figure 5. Setup for the garage packet reception ratio experiment.

Figure 6. Percentage of 15.4 packets correctly received, corrupted, and lost as the distance between 802.11 nodes and 15.4 nodes increases.

plication [16]. The sender's transmit power is set to 0 dBm and the packets are sent to the broadcast address. We use multiple receivers to minimize any receiver location-specific effects and hardware artifacts. Furthermore, the 802.15.4 receivers are configured to accept packets with CRC errors, while the transmitted packets have a predefined byte pattern to enable off-line bit error analysis for corrupted packets. Each receiver logs the entire packet contents for all incoming packets by transmitting them to a dedicated PC over its serial interface. Receivers also record whether a packet passed the CRC check. We use the set up described in Section 3.1 to acquire precise timing of all 802.11 and 802.15.4 packet transmissions. The DAQ card used for timing these transmissions is connected to the same PC used to log the 802.15.4 packets.

Figure 5 illustrates the relative positions of all the nodes used in this experiment. We examine the impact of different levels of 802.11 interference on the packet reception ratio (PRR) by varying the distance d between the 802.15.4 and 802.11 nodes. We run four sets of experiments with $d = 15, 65, 115, 170$ feet. For each value of d, we repeat the experiment using 802.11b and 802.11g radios. During each run, the 15.4 sender broadcasts 2,000 packets; with five 802.15.4 receivers, this corresponds to a total of 10,000 packet receive events under ideal conditions.

Results. We identify three types of 15.4 packet reception events: packets that are received correctly, packets that fail the CRC tests due to corrupted bits, and packets that are lost (i.e., transmitted but never received).

Figure 6 presents the relative percentages for each of these three events for different values of d. As expected, 802.15.4 PRR is significantly reduced due to 802.11 interference, especially when the two networks are closer to each other. As d increases, the 802.15.4 PRR improves since the 802.11 interference becomes progressively weaker.

We observe that 802.11b traffic has a much larger impact on the overall 802.15.4 PRR than 802.11g. Thonet et al. made a similar observation and suggested that this difference is due to the higher transmission rate of 802.11g networks, which lowers the channel-time for 802.11 packets [27]. We also observe, especially for smaller separations and 802.11b radios, that the number of lost packets is larger than the number of packets received with bit errors. This observation suggests that the front part of a 802.15.4 packet (i.e., the SHR) is more vulnerable to 802.11 interference, especially considering the relative sizes of the different packet parts. The second observation is important since it indicates that one needs
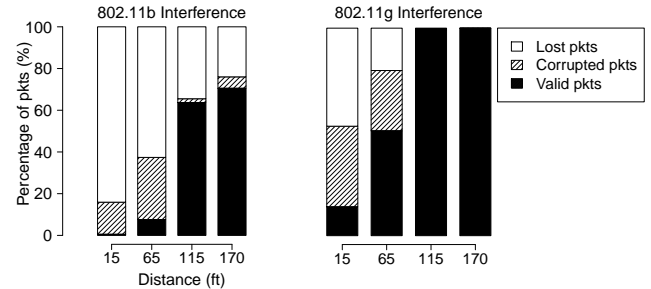
to focus on improving the detection of (partially) corrupted frames in order to improve the overall PRR. We return to this point in Section 3.4, where we present the distribution of bit errors over a 15.4 packet.

We also found that packet transmission latency increased by as much as 13% to 40% in the presence of 802.11g and 802.11b traffic respectively; another sign of the impact of 802.11 traffic on the 15.4 network. As discussed in Section 2, the 15.4 radio uses a CSMA/CA protocol where it performs a CCA check on the channel prior to each packet transmission. Since the 15.4 radio sends a packet only if the CCA check indicates a free channel, the latency of packet transmissions should increase in the presence of active 802.11 traffic.

Another interesting result is the impact of the 15.4 traffic on 802.11 throughput at $d = 15$ feet. We instrumented the 15.4 sender to transmit 10,000 128-byte packets at a rate of 75 ms, and the packet sniffer, `WireShark`, running on the 802.11 receiver recorded a 4% drop in TCP throughput.

3.3 Dynamics of 802.15.4 and 802.11 Interaction

To better understand the dynamics between the overlapping 802.11 and 15.4 networks shown in Figure 5 we examine next the RF activity logs captured during the experiments described in the previous section.

Figure 7 presents a timeline of 802.11b and 15.4 traffic activity when $d = 15$ feet (Figure 7(a)) and $d = 115$ feet (Figure 7(b)). Each vertical box corresponds to a single 15.4 broadcast, while the grey region corresponds to 802.11b activity, obtained from the narrow band radio as described in Section 3.1.

One can see from Figure 7(a) that 802.11 *backs-off* during 802.15.4 transmissions, when the separation between 802.11 and 802.15.4 nodes is small — an observation that contradicts the common belief that 802.11 nodes do not back off in the presence of 15.4 traffic [21]. We repeated the same experiment with five off-the-shelf 802.11b/g access points (from Apple, Belkin, Linksys, Netgear, and OpenMesh), and all exhibit the same behavior.

This behavior can be attributed to the 802.11 specification that mandates performing a clear channel assessment (CCA) prior to every data packet transmission. In other words, the 802.11b radio in our experiment sensed the channel noise floor being above the CCA threshold and deferred its pending transmission.
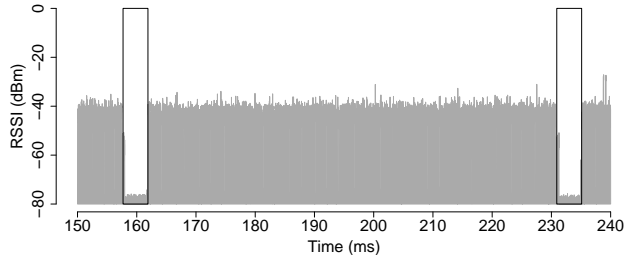
(a) $d = 15$ feet.
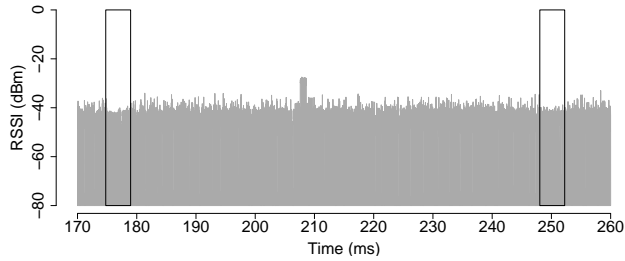
(b) $d = 115$ feet.

Figure 7. Overlay of 802.11b and 15.4 traffic. Each vertical box corresponds to a 15.4 packet transmission, while the gray lines are RSSI measurements corresponding to 802.11 transmissions. When d is small, the 802.11 radio backs-off when it senses a 15.4 transmission. As d increases, the 802.11 radio cannot detect 15.4 transmissions and packets collide.

We also note that in certain cases, the 802.11 radio will not back off. First, the 802.11 specification requires that RSSI ≥ -70 dBm for the channel to be considered busy when TX power ≤ 50 mW [10]. Second, the 802.11 specification lists three CCA modes (i.e., energy detection, packet detection, and both) and vendors can implement one or more at their discretion. 802.11 radios that use the packet detection CCA mode will declare the channel to be clear, since they cannot decode the overheard 15.4 packet transmission.

On the other hand, Figure 7(b) suggests that 802.11 does not back off when d is large. Nevertheless, due to the relatively high transmit power of 802.11 radios, the 802.11 transmissions can interfere with 802.15.4 transmission event at this distance (cf. Figure 6).

The discrepancy between 802.11 and 15.4 transmit powers leads to two distinct interference regions. In the *symmetric region* the signal from the 15.4 sender is strong enough to trigger the CCA check on the 802.11 transmitter. On the other hand, in the *asymmetric region* the 802.11 transmitter cannot detect 15.4 packets while it can still corrupt them.

We note that the 802.11 back-off behavior in the symmetric region seemingly contradicts the packet losses observed in Figure 6. Specifically, in the symmetric region, where 802.11 backs off due to ongoing 802.15.4 transmissions, we expect to see lower 802.11 interference compared to the asymmetric region. Instead, one can observe in Figure 6 that there is much larger 802.11 induced interference in this region as observed from the large number of lost and corrupted packets. The following sections examine and ex-
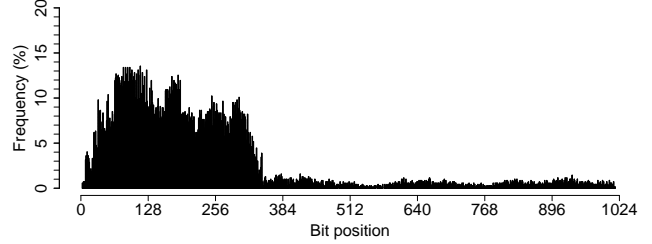
(a) 802.11b interfering source.
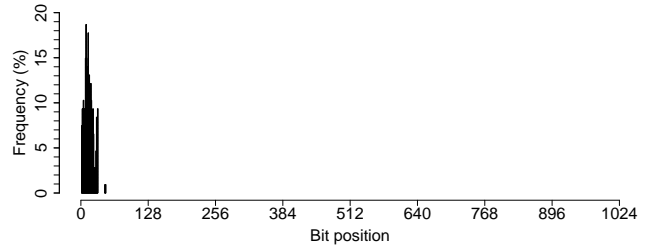
(b) 802.11g interfering source.

Figure 8. Bit-error distribution for 15.4 packets that failed the CRC check when the interfering 802.11 transmitter is in the symmetric region. It is far more likely that the front part of the 15.4 packet will be corrupted.

plain this apparently contradictory behavior.

3.4 802.15.4 Bit Error Distribution

To resolve the contradiction presented in the previous section, we examine the distribution of corrupted bits over 15.4 packets that failed the CRC check. Since we know the original packet content, it is possible to identify the bits that were corrupted during transmission.

First, Figure 8 shows the bit error distribution in the symmetric region. It is evident that the front section of a 802.15.4 packet has a much higher probability of incurring bit errors compared to the rest of the packet, which has almost zero bit errors. For now, let us sidestep the question why a collision happens in the first place and focus on the extent of the collision itself. Considering the relative durations of the 802.11 and 15.4 packets (cf. Table 1), the 802.11 transmission will finish well before the full 15.4 packet has been sent. At this point the 802.11 sender performs a CCA check, notices that the channel is busy, and defers any subsequent (re)transmissions. We note that in Figures 8(a) and 8(b) the extent of the corrupted packet region closely matches the duration of a single 1,500-byte 802.11b and 802.11g packet respectively.

Figure 9 illustrates this behavior in more detail, providing a zoomed-in view of the event timeline surrounding the transmission of a 15.4 packet. It is clear that once the first 802.11 packet collides with the 15.4 packet the 802.11 sender defers any subsequent transmissions until the end of the 15.4 packet. The initial transmission overlap generates the bit errors seen in Figure 8.

The large number of bit errors at the beginning of 15.4 packets can also explain the large number of missing packets as follows. As Figure 3 shows, the front part of the 15.4
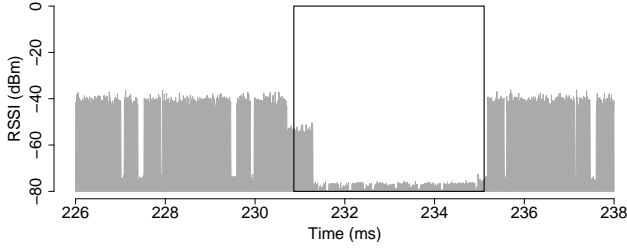
314

Figure 9. Detailed view of the 802.11b and 15.4 packet transmission timeline. The overlap at the beginning of the 15.4 packet (vertical box) corresponds to a collision with a 802.11 packet. The 802.11 sender defers sending any additional packets until the 15.4 transmission completes.
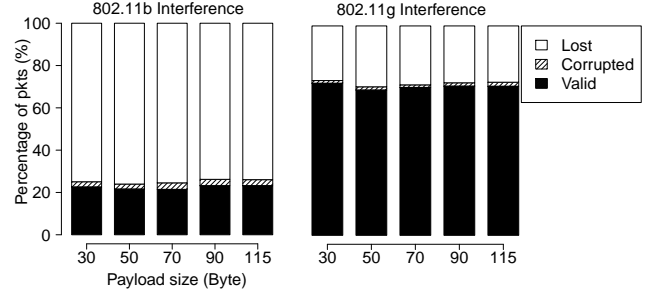

Figure 10. 15.4 packet reception rate as the payload size varies. The competing 802.11 sender lies within the symmetric region of the 15.4 sender. Since only bits in the front section of the 15.4 packet are corrupted varying the packet's length does not affect PRR.
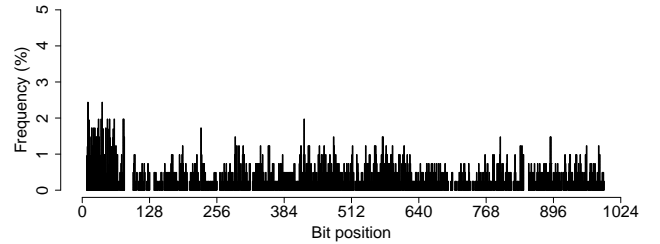

Figure 11. Bit-error distribution for 15.4 packets that failed the CRC check when the interfering 802.11g transmitter is in the asymmetric region. Bit errors are evenly distributed across the whole packet.

frame includes the SHR and PHR headers. Several problems can occur when the receiver cannot properly decode the SHR and the PHR. First, if the receiver cannot properly decode the Preamble or the SFD field, it will misinterpret the packet as channel noise. Second, if the Length field is corrupted the received packet will be either incomplete (when the decoded length field value is smaller than the actual packet length) or will contain additional junk bits (when the decoded length field value is larger). Both cases will result in a CRC failure.

The observation that bit errors are concentrated in the front part of the packet suggests that decreasing the size of the 15.4 packet will not increase the PRR. The results shown in Figure 10 confirm this hypothesis. As before, $d = 15$ feet, but the 15.4 sender broadcasts packets with payload sizes 30, 50, 70, 90, and 115 bytes. Despite a three-fold increase in payload size the PRR remains effectively constant.

We can now explain why 15.4 and 802.11 packets collide. Looking at Figure 4, the only time that a 15.4 sender can begin its transmission is during the DIFS + Contention Window period since it otherwise senses the channel as busy. Furthermore, the time granularity that the 15.4 sender senses the medium is equal to the slot time (= $320\ \mu$s) and it senses the medium for eight symbol periods (= $128\ \mu$s) before declaring the channel as idle [9]. Considering the short length of the DIFS interval and the shorter 802.11 slot time (cf. Table 1) it is very likely that during the time the 15.4 sender senses the channel, the 802.11 node also senses the channel. As a result of both nodes sensing the channel idle, they start transmitting at the same time and subsequently collide.

Finally, Figure 11 shows the 802.15.4 packet bit error distribution in the asymmetric region. Compared to results in the symmetric regions, bit errors are almost uniformly located throughout the 15.4 packet. We note that the lack of bit errors near the end of the packet in the figure is partly due to the corrupted length field.

The difference in the bit corruption patterns seen in the two regions implies that we need to develop different techniques, targeting individual regions, to overcome the negative impact of 802.11 traffic on 15.4 transmissions.

So far we have shown aggregate statistics about which bits in the 15.4 frame are more likely to be corrupted in the two regions. We are also interested in the number of cor-

rupted bits and their distribution over individual 15.4 packets since this information will be useful in designing protection mechanisms. Figure 12 presents the CDF of the total number of corrupted bits in both regions for 802.11b and 802.11g senders. Interestingly, corrupted 15.4 packets received in the symmetric region have a wider spread in the number of corrupted bits, and they are also more severely damaged than corrupted packets received in the asymmetric region.

While Figure 12 presents the number of corrupted bits, Figure 13 presents the density with which these bits appear over the 15.4 packet. Specifically, it plots the probability density function of the distance n between any two corrupted bits in the packet. Small values of n correspond to bursts of corrupted bits, while corrupted bits randomly scattered throughout the header will result in large values of n. We can see from this figure that errors occur in bursts, especially in asymmetric regions. This corresponds to, possibly multiple, 802.11 packets colliding with the 15.4 packet.

4 Protecting 15.4 packets from WiFi senders

Based on the insights from the above measurements, we design targeted redundancy mechanisms to compensate WiFi interference. Depending on whether the ZigBee node can push back the WiFi transmissions, we investigate techniques for symmetric and asymmetric regions respectively.

4.1 Symmetric Region Techniques

Section 3 shows that in the symmetric region corrupted bits occur at the front of a 15.4 packet. Such corrupted pack-
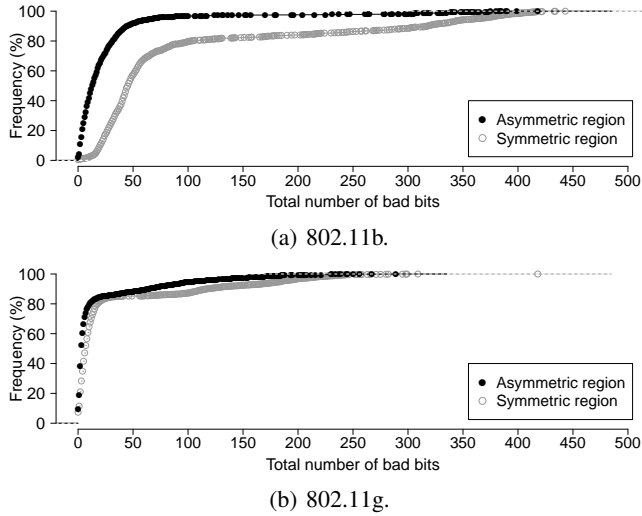
(a) 802.11b.

(b) 802.11g.

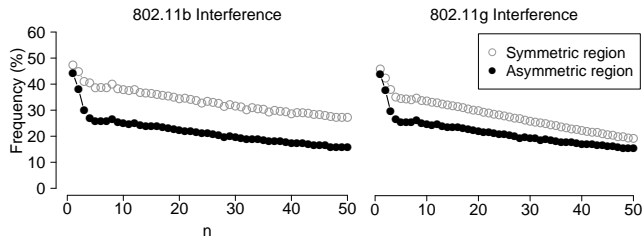**Figure 12. CDF of the number of bad bits in a corrupted packet.**

Figure 13. Distance n between any two corrupted bits in a 15.4 packet. Errors caused by competing 802.11b and 802.11g senders occur in concentrated bursts.
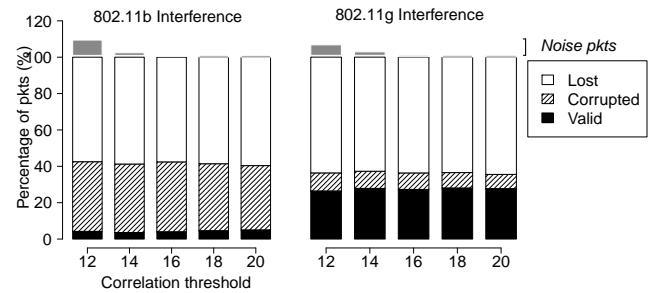

Figure 14. 15.4 PRR in the presence of 802.11b interference as the TI CC2420 correlation threshold varies. Lower threshold values do not increase PRR but lead the receiver to incorrectly decode channel noise as packets.
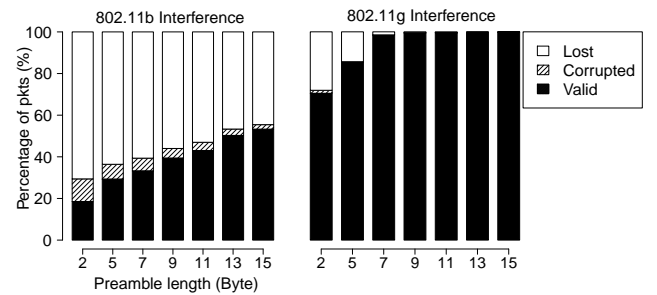

Figure 15. 15.4 PRR as the preamble length varies. Due to the shorter 802.11g packets it is possible to recover all 15.4 frames by increasing the preamble's length.

ets are traditionally recovered through an Automatic Repeat Request (ARQ) protocol. For example, the Collection Tree Protocol (CTP), a widely used protocol in the WSN community, uses hop-by-hop retransmissions aggressively [3]. Even though ARQ improves the packet reception ratio, it does so at the expense of higher energy consumption and lower channel throughput.

Considering that only the front section of the packet is corrupted and that a large portion of packets may not be affected by interference, retransmitting the same packet multiple times is intuitively inefficient. In this section we investigate whether it is possible to overcome this specific form of packet corruption without retransmissions. We start with two straw man approaches that provide the desired outcome only partially and conclude with a simple, yet efficient mechanism that does.

4.1.1 Correlation Threshold

As we described in Section 2, some 15.4 radios provide a user-defined *correlation threshold* that determines the amount of noise that the radio is willing to tolerate when decoding incoming 32-chip sequences in searching for the SHR. Considering that WiFi interference is a form of (non-random) noise, it is then plausible that varying the correlation threshold will increase the PRR.

We tested the effectiveness of this technique by varying

the correlation threshold of a CC2420 receiver. In this case, the maximum correlation threshold is 32 and the default is set to 20. While operating in the symmetric region, we varied the correlation threshold from 12 to 20 in increments of 2 and logged the received packets. Figure 14 presents the results of this experiment. Decreasing the threshold does not increase the number of correctly received packets. The only change is a negative one: increasing the instances in which the 15.4 radio mistakenly interpreted background or WiFi-related noise as the start of a valid 15.4 packet.

4.1.2 Preamble Length

While the 15.4 specification mandates a 4-byte preamble, radios such as the CC2420 allow the user to set the length of the transmitted preamble up to 17 bytes. We leverage this capability to overcome the effects of 802.11 interference on 15.4 packets as follows. Consider an instance for which the WiFi and 15.4 packets overlap by n 15.4 bytes. Then, if the preamble's length was $n + 4$ bytes, the receiver would be able to properly decode the preamble's last four bytes to receive the packet correctly.

To verify that a longer preamble does indeed reduce packet loss in the symmetric region, we ran an experiment in which we varied the preamble length and observed the packet reception ratio. Figure 15 illustrates the experiment's results. As expected, increasing the preamble length increases the PRR. Nevertheless, this technique has two drawbacks. First, the maximum preamble length that the CC24240 radio supports is 17 bytes. This preamble length cannot fully protect a
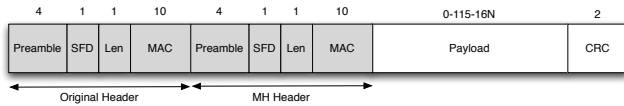
Figure 16. MH: a 15.4 packet with an additional header.

	15.4 header	Additional headers		
		1st	2nd	3rd
TCP	30.5%	49.5%	10.0%	1.9%
UDP	28.2%	53.9%	12.9%	1.8%

Table 2. Percentage of packets successfully received using the original 15.4 header or one of the additional headers.

15.4 packet from all WiFi packets, since such transmissions can take more than 480 μs (cf. Table 1). Second, since the 15.4 specification requires a four-byte preamble, other 15.4 radios, such as the Atmel RF230 [1], do not support variable-length preambles.

4.1.3 Multi-Headers

Next, we introduce *Multi-Headers* (MH), a light-weight sender-initiated mechanism that emulates the PRR improvements due to longer preambles, but is effective against a wider range of competing WiFi packets.

The naïve approach to emulate the effect of longer preambles is to send two packets back-to-back. The first packet, whose sole purpose is to save the second packet from corruption, carries a dummy payload to make the 802.11 back off. The following packet can then be correctly received with higher probability. Unfortunately, it can be difficult to transmit back-to-back packets. For example, the smallest inter-packet interval with TelosB motes is as high as 600 μs, considering the time to send the STXON or STXONCCA command over the SPI bus and the 12 symbol periods that the CC2420 radio waits before each transmission.

Rather than transmitting multiple packets, MH transmits multiple packet headers back to back. Such transmission of consecutive headers is feasible due to the much simpler packet decoding approach that 15.4 radios use, compared to 802.11 radios. Specifically, 802.11 b/g radios use different modulation schemes and transmission rates for the packet header and the payload. This feature allows 802.11 radios to detect and switch to a stronger new packet transmission in the middle of a weaker packet transmission and overcome hidden terminal effects. Furthermore, this approach enables backward-compatibility with older 802.11 standards. On the other hand, 15.4 radios transmit the whole packet with the same modulation scheme and bit rate. Once the 15.4 receiver correctly detects the SHR and PHR headers, it continues to decode the incoming RF signal until it receives the number of bytes mentioned in the PHR header. This feature implies that we can safely add multiple headers within a single 15.4 packet and the receiver will treat them as part of the payload.

Figure 16 shows a legitimate 15.4 packet with one additional set of headers in the payload. Given this two header packet structure, if there are no overlapping 802.11 transmissions, the receiver will detect the first SFD after the first preamble sequence and will treat this SFD as the start of the packet; the radio treats the second packet header as a part of the payload. On the other hand, if the first preamble bytes were corrupted due to an overlapping 802.11 transmission, the 15.4 receiver may not detect the first SFD correctly; instead, the receiver will detect the second SFD preceded by four preamble bytes and assume the packet starts at the second SFD.

With multiple packet headers per packet, the length field

of each header must be properly adjusted. For example, in Figure 16, the length field of the second header corresponds to the length of the actual payload, while the length field of the first header is higher by 16 bytes. Given that the radio treats additional headers as payload, the receiver's software stack needs to remove any remaining headers from the payload before delivering the packet to the user application.

The CRC in the 15.4 packets covers both the header and payload, which limits its applicability in the presence of MH. Specifically, depending on the header detected by the radio, the 15.4 header and payload will be different. To address this problem, we disable the 15.4 CRC filtering on the radio and modify the radio software stack to include a 2-byte CRC within the packet's payload. This CRC covers the innermost header (excluding the length field) and the user payload.

Evaluation. We evaluated the effectiveness of MH using the following experimental setup. Five 802.11g clients were connected to the same AP in infrastructure mode to simulate a typical office setting. These 802.11g clients sent TCP and UDP traffic as fast as possible to the PC connected to the AP via an Ethernet cable. The 802.11g clients were distributed within the same office and the 15.4 sender was 15 ft away from four 15.4 receivers. Activity traces of the 802.11g activity collected by the ML2724 radio verified that the 15.4 sender was within the symmetric region. The 15.4 sender broadcasted 2,000 128-byte packets at a rate of one packet per 75 ms and it filled the packets payloads with four additional in-payload headers and a 50-byte application payload. In addition, for each header, we replaced the source address field in the 15.4 header with a counter that acts as a header index for offline analysis.

Table 2 shows the number of successfully received packets as triggered by each additional header. Having even a single additional header increases PRR by 50%. The benefit of MH diminishes as we increased the number of additional headers beyond one, suggesting that two headers in total are sufficient. Achieving an effective PRR of 80% to 82.1% (compared to the original 28%-30%) outweighs the 20% packet overhead incurred by the one additional header. Finally, we note that we observed similar performance for 802.11b traffic.

4.2 Asymmetric Region Techniques

The results in Section 3 showed that *symmetric* and *asymmetric* regions lead to two distinct bit error patterns. Bit errors in the asymmetric region, in contrast to the symmetric region, are uniformly distributed across the packet. Therefore, MH, that protects only the packet header cannot protect from these bit errors.

Packet loss due to bit errors is resolved using either ARQ or Forward Error Correction (FEC). Although packet retransmission is commonly used under low to moderate packet

loss, FEC is more suitable to overcome packet loss under heavy interference for the following reason. Under heavy interference, a packet has to be retransmitted many times, which induces extra energy cost for the motes and increases channel congestion.

FEC augments each packet with extra information that enables the receiver to correct some of the bit errors. Although FEC algorithms are widely used in digital communications, selecting the right algorithm and implementing it on resource-constrained sensor nodes are non-trivial. In this section we evaluate several FEC techniques, in terms of their error recovery performance and implementation overhead.

4.2.1 Error-Correction Codes

An FEC transmitter applies an Error-Correction Code (ECC) to the data to be transmitted. The ECC transforms the message to a larger encoded message. The receiver then applies the reverse transformation to recover the original message from the encoded message. The redundancy in the encoded message allows the receiver to recover the original message in the presence of a limited number of bit errors.

One example of an ECC is the linear code that the 15.4 physical layer employs to overcome RF noise [9]. As mentioned in Section 2.1, the 15.4 radio maps 4-bit symbols to 32-bit chip sequences. Since the minimum Hamming distance among the sixteen predefined chip sequences is 12, if the received chip sequence does not have bit errors at more than 6 positions, the 15.4 radio can properly map it to the correct chip sequence. However, we argue that the 15.4 ECC is not sufficient against external 802.11 noise, which typically lasts longer than six chip times, or 3 μs.

Next, we evaluate two ECCs, namely the Hamming code and the Reed-Solomon code for correcting 802.11-induced bit errors on 802.15.4 packets.

4.2.2 Hamming Code

Hamming codes enable FEC by adding extra parity bits to the message. They can detect up to two bit errors and correct one bit error in the encoded message. In particular, we use the Hamming(12,8) code, in which four parity bits are added to every eight bits of data to generate encoded messages that are 12 bits long. The Hamming(12,8) code can detect and correct one bit error within the 12 bit word. If more than one bit errors are present, the decoded message will most likely correspond to a data word other than the original. This implies that, once a message with unknown number of bit errors is decoded, the validity of the decoded message has to be verified by some other techniques such as a CRC check.

We implemente a Hamming(12,8) code-based FEC to recover 802.11-induced 802.15.4 packet errors. Our implementation uses 72-byte messages, which results in 108-byte encoded messages (we packed two 12-bit encoded values to three bytes). The 72-byte message contains a 2-byte CRC field to verify the messages correctness after the Hamming decoding. This implementation uses 754 bytes of ROM (excluding the CRC code) and 82 bytes of RAM (excluding the data and encoded message buffers). Encoding and decoding the 108-byte messages requires 1.4 ms and 1.8 ms respectively on a TelosB mote running at 4 MHz.

Our implementation places each 12-bit encoded message in consecutive locations in the 108-byte packet payload.

	Hamming(12,8)		Hamming(12,8) w/ Bit interleaving		RS w/ 30-byte parity	
	11b	*11g*	*11b*	*11g*	*11b*	*11g*
15 ft	0.6%	11.7%	12.4%	57.6%	52.0%	65.2%
65 ft	4.7%	19.1%	55.6%	70.4%	85.3%	85.9%

Table 3. Percentage of corrupted packet payloads that can be recovered by two version of the Hamming code and the RS code.

Encoding	Decoding		
	15-byte error	*30-byte erasure*	*no errors*
36.156 ms	181.892 ms	207.824 ms	104.296 ms

Table 4. Execution time for TinyRS operations. The original message is 65 bytes long and the RS-encoded message contains the original 65-byte message and the 30-byte parity.

Hence, all the 12 encoded bits are transmitted as consecutive bits in the radio packet. While the Hamming(12,8) code is very efficient in terms of execution cost and memory overhead, the first column of Table 3 shows that only a very small fraction of the corrupted messages are recovered by the Hamming(12,8)-based FEC scheme. Its poor performance is due to the burstiness of bit errors (see Figure 13), which results in more than one bit error within an encoded message thus preventing correct error recovery.

Next, we apply bit interleaving to make the encoded message more resilient to bursty errors. Our implementation treats the 108-byte encoded messages as a (108 × 8) sequence of bits. For each 12-bit encoded message, we evenly spread each bit over the entire message (i.e., two consecutive bits in the 12-bit message are separated by 72 bits in the interleaved message). Interleaving is reversed during the decoding process by concatenating 12 bits, evenly spread across the message, to form the 12-bit encoded message.

The second column of Table 3 shows the error recovery performance of the bit interleaved Hamming encoding. Due to the heavy use of the bit-level operations, the execution times for encoding and decoding a 108-byte message now become 6.7 ms and 9.2 ms respectively. The implementation consumes 1.4 KB of ROM and 0.1 KB of RAM space.

4.2.3 Reed-Solomon Code

The Reed-Solomon (RS) code is a block-based linear error-correction code with a wide range of applications in digital communications and storage. Unlike the Hamming code, the RS code can recover from both data corruptions and erasures; the former refers to bit flipping at *unknown* positions in the packet, while the latter refers to missing pieces of data at *known* locations. The RS code divides a message into x blocks of user-defined size and computes a parity of y blocks. An RS-encoded message then consists of the original message and the computed parity. The length of the parity determines the maximum number of corrupted and erasure blocks in the encoded message that the receiver can successfully recover from. Specifically, for y blocks of parity, the number of erasure and corrupted blocks that the RS code can recover from is:

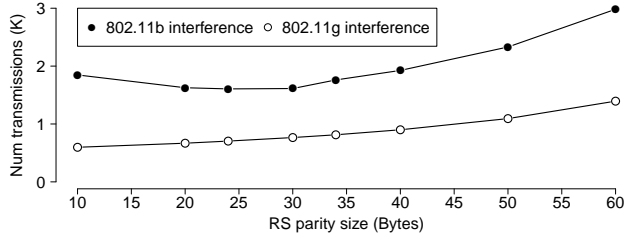$$2 \times (num\_corrupted\_blks) + 1 \times (num\_erasure\_blks) < y$$

Figure 17. Total number of 15.4 transmissions necessary to transfer a 38-KB object over a single hop in the presence of interference from 802.11 traffic.

The RS code is commonly (mis-)believed to be too computationally and memory intensive for resource-constrained motes [13]. Previous work minimizes the implementation complexity by either implementing only the encoding engine [24], or focusing on recovering from data erasures only [14]. However, since a corrupted length field can mislead the radio into demodulating a smaller packet, we argue that it is advantageous to handle both data corruptions and erasures. To this end, we have developed a full-featured TinyOS-compatible RS library, *TinyRS*, based on the work of Karn et al. [19]. The rest of this section outlines the performance of RS code based on our TinyRS implementation.

TinyRS has a relatively small code footprint, requiring 2.9 KB of ROM and 1.4 KB of RAM when using 8-bit block size and 30-byte parity. Table 4 presents the micro-benchmark on the execution time in the case of a 65-byte message. The encoding time is significantly lower than the decoding time and the latter also depends on the state of the received RS-encoded message. In Section 5, we further describe a real-world system that attempts to reduce the impact of decoding overhead on network throughput.

The third column of Table 3 illustrates the benefits associated with the increasing processing overhead: RS can successfully recover four times more packets than Hamming(12,8) with bit interleaving, when 15.4 packets are corrupted by an 802.11b transmitter in the symmetric region.

Using larger parities increases the probability of recovering bits corrupted by interference, thereby decreasing the need for retransmissions. At the same time, larger parity decreases the space in the 15.4 payload that can be used to deliver application data, leading to more packet transmissions.

To guide the decision on the parity size, we ran simulations to determine the expected number of transmissions necessary to deliver a 38-KB object over a single hop for various parity sizes. To do so, we first obtained the link's effective PRR by simulating the transmission of 10,000 RS-encoded packets with various parity sizes and applying the bit errors observed in the packet traces from Figure 6 (68 ft.). We calculated the effective PRR for each parity size by counting both valid packets and corrupted packets that RS can successfully recover. From the effective PRR we calculate the expected number of transmissions to deliver a 38-KB object, shown in Figure 17. The results suggest that the 30-byte parity requires the smallest number of transmissions.

Finally, to further illustrate the effectiveness of TinyRS in reducing the expected number of transmissions, we consider two other packet recovery strategies: packet-level and block-level ARQ. Both approaches rely on acknowledgments to decide whether to initiate retransmissions. However, block-level ARQ divides a packet into sub-blocks and allows the sender to retransmit only the corrupted blocks [5]. For simplicity, we assume that the network can always successfully delivery acknowledgement packets. In the scenario of delivering a 38-KB object mentioned before, packet-level ARQ would need to transmit a total of 4,409 packets, while block-level ARQ (with 30-byte blocks) would require a total of 2,313 packets. In comparison, with 30-byte parity, TinyRS transmits only 1,720 packets. However, TinyRS requires additional energy to encode and decode payload. In the previous example, each RS-encoded packet would use an additional 0.435 mAs for encoding and decoding packets with 15 or less bit errors on a 4 MHz TelosB mote, or 748 mAs for 1,720 packets. This is in comparison to 1,290 mAs and 284 mAs used by the additional transmissions in packet-level and block-level ARQ (considering both sending data packets and waiting for acknowledgements). If we consider that acknowledgements could be lost, we expect the ARQ methods would use even more energy.

5 BuzzBuzz MAC Layer

The results from Sections 4.1 and 4.2 show that MH and TinyRS improve the 802.15.4 PRR in the presence of 802.11 interference. MH improves the detection of packets by protecting the packet header, while TinyRS protects against bit errors in the packet payload. This section presents *BuzzBuzz*, a MAC-layer solution that combines MH and TinyRS to improve the overall PRR under 802.11 interference. Experimental results from a 57-node testbed show that BuzzBuzz improves the end-to-end data yield of the CTP data collection protocol, while reducing the overall network traffic by 71%, under severe 802.11 interference.

5.1 BuzzBuzz Protocol Design

When designing a networking solution, it is important to identify the best architectural layer at which it should operate. We argue that both MH and TinyRS are best positioned at the MAC layer due to the following reasons.

First, the MAC layer typically maintains neighborhood and link quality information that BuzzBuzz can leverage to improve the packet delivery efficiency. For example, depending on the link quality, BuzzBuzz can decide if the overhead of running the error correction code is justified. BuzzBuzz can also leverage the MAC layer's knowledge of the underlying radio header format to construct MH headers.

Second, while running FEC only at the source and the destination nodes of a multi-hop path reduces the computation cost, the bit errors accumulated over the intermediate hops will reduce the likelihood of successfully decoding the packet at the destination. Therefore, we optimize FEC operations for the MAC layer and perform packet encoding and decoding on every hop along the end-to-end path.

ARQ is the most widely used approach in WSNs to implement reliable delivery at the MAC layer. In ARQ, the sender retransmits a packet if the receiver has explicitly (i.e., negative acknowledgement) or implicitly (i.e., the lack of acknowledgement) indicated that the current packet is lost.

319

BuzzBuzz complements ARQ with the selective use of MH and TinyRS. The three techniques (i.e., MH, TinyRS, and ARQ) present different trade offs. Although ARQ has the least space and computational overhead, it is not efficient in very noisy environments. Similarly, MH has less computational overhead than TinyRS, but is less effective in the asymmetric region. The main challenge that BuzzBuzz addresses is deciding which of these techniques is appropriate given the current link quality.

One can use RSSI samples, collected over a period of time, to detect external channel interference. Musăloiu-E. et al. proposed three aggregation functions to analyze RSSI measurements in real time and detect noisy 15.4 channels [18]. Since interference levels and channel conditions change over time, motes need to periodically sample the channel in that approach. Periodic sampling of RSSI may not be suitable for all the systems, especially those that use low-power duty-cycling.

Instead of periodic sampling, BuzzBuzz infers the channel quality by observing the packet losses, or the lack of packet acknowledgments. Upon receiving a packet from the upper layer, the BuzzBuzz sender first attempts to deliver the packet using ARQ. If the packet cannot be successfully delivered after three attempts, the BuzzBuzz sender adds the FEC information, and inserts one MH header in the packet. The sender then makes three more transmission attempts of the encoded message before giving up. We note that the BuzzBuzz sender explicitly indicates that a packet contains the FEC parity by setting the reserved bit 7 in the Frame Control Field (FCF) of the 15.4 frame to 1. In addition, to help the receiver locate the application payload, the reserved bit 8 in the FCF of the last MH header is set to 1.

The two-phase retransmission approach has the advantage of avoiding the overhead of MH and TinyRS when external interference is low. On the other hand, in environments with persistent interference, performing the two-phase probing for each packet slows down the transmission as the initial ARQ phase will most likely fail. To address this problem, BuzzBuzz remembers the setting of the last packet transmission for 60 seconds and applies it to the next packet transfer. The sender falls back to the naive retransmission scheme after receiving three consecutive packets that pass the MH CRC. The receiver piggy-backs this information in its acknowledgments.

The results from Section 4.2 show that TinyRS requires at least 150 ms to decode a 95-byte RS-encoded packet. This decoding time dominates the processing delay during packet reception. This computational overhead is incurred even when the RS-encoded packet does not have any bit errors. BuzzBuzz uses the CRC field of the packet (cf. Section 4.2) to reduce the decoding overhead when the packet is received with no bit errors. Specifically, BuzzBuzz uses CRC to check the integrity of the payload, and attempts decoding only if the CRC check fails. CRC can be efficiently implemented with lookup tables, and computing CRC over 65-byte application payload takes approximately 325 μs.

5.2 Evaluation

To evaluate BuzzBuzz, we integrated it with the `PacketLink` component in TinyOS 2.1. As mentioned in

	CTP	CTP w/ BuzzBuzz
Packet Delivery Rate	43.05%	73.90%
Avg number pkts/s in the network	38	11
% pkts not ACKed	66%	35%
% pkts received due to MH hdr	N/A	10.58%
% corrupted pkts recovered with RS	N/A	42.69%
% decrease in 802.11g throughput	14.51%	3.35%

Table 5. Summary of experiment results running CTP with BuzzBuzz on a 57-node testbed.

Section 2.1, the CSMA/CA protocol implemented in TinyOS uses a fixed-length backoff interval. We ran experiments on a 57-node TelosB testbed deployed in an office building. All nodes were tuned to 15.4 channel 16. We decided to use a real testbed, because simulators such as TOSSIM do not fully simulate the 15.4 modulation/demodulation scheme and can not match the full realism of testbeds.

Since data collection applications dominate real-world WSN deployments, we developed a simple application that uses the Collection Tree Protocol (CTP) [3] to deliver 65-byte application data from each node at a rate of one packet per minute. CTP relies on acknowledgments and packet retransmissions to improve the packet delivery rate.

The 802.11 interference originated from a co-located 802.11g testbed on the same building floor. The 802.11g testbed backbone consisted of six OpenMesh OM1P mesh routers forming an ad-hoc mesh backbone on 802.11 channel 5, with one node acting as the gateway between the 802.11 mesh and an Ethernet network. Three Nokia N800 Internet tablets used the OpenMesh network to continuously send TCP traffic to a PC on the same Ethernet network as the OpenMesh gateway.

To ensure that CTP had sufficient time to build its routing tree, we started the 802.11g traffic 20 minutes after the start of the 15.4 nodes. Each experiment lasted two hours. We evaluate the effectiveness of BuzzBuzz using the end-to-end CTP data delivery ratio (or goodput), and the amount of 15.4 network traffic.

Table 5 presents the average results from two experiment runs. CTP with BuzzBuzz is able to deliver 71% more packets while reducing the network traffic by two third. Note that since all data packets carry a 65-byte application payload, the packet delivery rate can be translated into effective data delivery rate. The difference in the amount of network traffic is due to the aggressive retransmissions that CTP uses for unacknowledged packets. Specifically, a CTP node can attempt up to 30 retransmissions before discarding the packet. Since the probability of packets having at least one bit corruption is high in the presence of 802.11g traffic, many retransmissions are needed for a successful packet delivery. The effectiveness of BuzzBuzz is also evident from the fact that it reduces the number of packets not acknowledged by 50%.

The middle part of Table 5 presents the contributions from each of the two BuzzBuzz components. Approximately 10% of all packets received (valid or corrupted) were due to the MH header being detected by the radio. With a 30-byte parity, TinyRS was able to successfully recover approximately 42% of the corrupted packets. Finally, Table 5 shows that

BuzzBuzz has a lower impact on the 802.11g throughput; a 3.35% decrease as compared to 14.56% decrease in the case of CTP. This improvement is due to the fewer 15.4 packets generated in the case of CTP with BuzzBuzz.

6 Future Directions

We have shown that BuzzBuzz achieves significant improvements over transmitting raw packets. These results lead to several future directions of research.

Network-wide blocker. BuzzBuzz is a reactive approach. Each ZigBee node operates independently to mitigate WiFi interference. Leveraging the observation that 802.11 nodes back off during active transmissions from nearby 15.4 nodes, it is possible to design *proactive* solutions for dense ZigBee networks. The idea is to use a collection of dedicated *802.11 blockers* placed close to each 802.11 node. While there are implementation challenges, such as the explicit coordinations among the blockers and between blocks and communicating 15.4 nodes, we ran a simple experiment with one 15.4 blocker placed next to the 802.11 access point to evaluate the feasibility. And, we observed an increase in 15.4 throughput by as much as 26%.

Performance under 802.11n interference. The 802.11n standard introduces several new features not present in 802.11b/g. However, these features do not completely mitigate the CTI problem between 15.4 and 802.11 networks, making BuzzBuzz still relevant when mitigating WiFi interference.

With 802.11b and 802.11g, we observed that higher bit rates make WiFi more responsive when backing off during 802.15.4 transmissions. Although the 802.11n standard supports higher bit rates, our preliminary results show that the 15.4 PRR in the presence of 802.11n traffic increased by only 3%, compared to under 802.11g interference.

Furthermore, channel bonding is a mechanism that combines two adjacent 802.11 channels to create a wider channel for higher throughput. As discussed earlier, current 15.4 deployments typically make use of *interference-free* channels that do not overlap with occupied 802.11 channels as a technique to avoid 802.11 interference. However, with channel bonding, many of these interference-free channels will now be under 802.11n interference.

7 Related Work

The WSN community has acknowledged the impact of 802.11 interference on WSN applications in various settings. Ko et al. collected empirical results in a hospital setting where they found that running CTP on a 15.4 network that overlapped with an active 802.11 channel decreased the end-to-end goodput by a factor of three [15]. Hauer et al. studied the impact of 802.11 interference on body sensor networks and found that the position of bit errors in 15.4 packets are temporally correlated with 802.11 traffic [6]. Hou et al. observed a 15.4 packet loss as high as 87%, with an 802.11b sender located in between two 15.4 nodes five meters apart [7].

The common approach to mitigate 802.11 interference on 15.4 networks is to switch the network to channels that do not overlap with an active 802.11 channel. Musăloiu-E. and Terzis [18] proposed a distributed channel selection mechanism that detects 802.11 interference using periodic RSSI samples. Unfortunately, 802.11-free 15.4 channels may not always be available. Outside of Japan, only 15.4 channels 25 and 26 do not overlap with any of the 802.11 channels. These two channels may not be sufficient to accommodate multiple collocated 15.4 networks, or high-throughput applications [16]. Kannan et al. proposed an off-line strategy to quantify the level of link burstiness due to interference, known as the β-factor, from RSSI traces [25]. 15.4 nodes then use this information to estimate the expected duration of the interference and defer outgoing packet transmissions to reduce the retransmission cost. However, with 802.11-enabled mobile devices, the 802.11 interference pattern may change dramatically in a short time, making off-line approaches less effective. More recently, Boano et al. [2] simulated general 2.4 GHz interference using CC2420 radios in an effort to identify mechanisms that can improve the robustness of existing MAC protocols under 802.11 interference. We investigate WiFi interference with a more persistent presence and heavy traffic. Instead of deferring, our work aims to increase the PRR of 15.4 networks by being more resilient to 802.11 interference.

Hou et al. proposed integrating an 802.11 radio chip on a 15.4-enabled medical device [7]. Before the device transmits a 15.4 frame, it sends out an 802.11 RTS packet to reserve the channel, preventing nearby 802.11 radios from sending traffic. BuzzBuzz does not require any additional hardware.

While early work from the 802.11 community concluded that 15.4 radios have little impact on 802.11 radios [8], more recent work has amended this view. Gummadi et al. reported that 15.4 signals can lower 802.11 SNR, significantly impacting the 802.11 throughput [4]. Furthermore, Pollin et al. showed that, despite 15.4 radios exercising carrier sense, 15.4 traffic can still collide with 802.11 transmissions and lower 802.11 throughput [21]. We are the first to examine these interactions at a finer granularity and found two distinct modes of 15.4 and 802.11 interference.

The wireless community has recently proposed methods to efficiently recover from packet corruption. Lin et al. proposed ZipTx that uses the RS code in 802.11 networks to reduce the retransmission costs. In addition to the RS code, BuzzBuzz tries to minimize the number of erasure packets though MH. Instead of relying on computation-intensive RS code, Maranello applies CRCs on blocks of the payload [5]. Then, based on the CRC validation feedback messages, the sender retransmits only the corrupted data blocks. However, efficiently sending feedback messages on a noisy channel can be difficult. In addition, the trace-driven simulations in Section 4.2.3 show that such a block-CRC approach may not efficiently solve the coexistence problem between 15.4 and 802.11 networks. Jamieson et al. proposed Partial Packet Recovery (PPR) that replicates the packet header at the end of 802.11 packets [12], but PPR requires the use of software radios and does not work on existing 802.11 hardware. Finally, Bluetooth uses a $\frac{1}{3}$ rate FEC to protect the packet header from bit errors by repeating each bit three times [11]. On the other hand, MH replicates both the packet header and preambles to improve detecting incoming packets.

8 Conclusion

This papers presents a careful analysis of the IEEE 802.15.4 and 802.11 interference patterns at 2.4 GHz ISM band. We examine these interference patterns at a bit-level granularity, and we explain how a 15.4 node may change the behavior of nearby 802.11 transmitters under certain conditions. With these observations, we define the symmetric interference regions and asymmetric regions. This paper then presents BuzzBuzz, a MAC layer solution that enables 15.4 nodes to coexist with WiFi networks. BuzzBuzz uses Multi-Headers (MH) and Forward Error Correction (FEC) to overcome the packet loss due to 802.11 interference. We implemented TinyRS to show that a full-featured FEC library is feasible on resource-constrained motes. We observe that BuzzBuzz increases the packet reception rate on a 57-node testbed by 70%, while simultaneously reducing the number of 15.4 transmissions by a factor of three.

Finally, we note that although our current solutions are software implementations running on the microcontroller attached to the 15.4 radio, they can be implemented more efficiently on the radio chip itself. We hope that this paper will act as a guidance for future 15.4 radio designs that can withstand 802.11 interference.

Acknowledgments

9 References

[1] Atmel Corporation. Low Power 2.4 GHz Transceiver for Zig-Bee, IEEE 802.15.4, 6LoWPAN, RF4CE and ISM applications. Available at http://www.atmel.com/dyn/resources/prod_documents/doc5131.pdf, 2009.

[2] C. A. Boano, T. Voigt, N. Tsiftes, L. Mottola, K. Romer, and M. A. Zuniga. Making Sensornet MAC Protocols Robust Against Interference. In *EWSN*, 2010.

[3] O. Gnawali, R. Fonseca, K. Jamieson, D. Moss, and P. Levis. Collection Tree Protocol. In *SenSys*, 2009.

[4] R. Gummadi, D. Wetherall, B. Greenstein, and S. Seshan. Understanding and Mitigating the Impact of RF Interference on 802.11 Networks. In *SIGCOMM*, 2007.

[5] B. Han, A. Schulman, F. Gringoli, N. Spril, B. Bhattacharjee, L. Nava, L. Ji, S. Lee, and R. Miller. Maranello: Practical Partial Packet Recovery for 802.11. In *NSDI*, 2010.

[6] J.-H. Hauer, V. Handziski, and A. Wolisz. Experimental Study of the Impact of WLAN Interference on IEEE 802.15.4 Body Area Networks. In *EWSN*, 2009.

[7] J. Hou, B. Chang, D.-K. Cho, and M. Gerla. Minimizing 802.11 Interference on Zigbee Medical Sensors. In *BodyNets*, 2009.

[8] I. Howitt and J. Gutierrez. IEEE 802.15.4 Low Rate - Wireless Personal Area Network Coexistence Issues. In *WCNC*, 2003.

[9] IEEE Computer Society. 802.15.4: Wireless Medium Access Control (MAC) and Physical Layer (PHY) Specifications for Low-Rate Wireless Personal Area Networks (LR-WPANs). Available at: http://standards.ieee.org/getieee802/download/802.15.4-2003.pdf.

[10] IEEE Computer Society. Local and metropolitan area networks - Specific requirements Part 11: Wireless LAN Medium Access Control (MAC) and Physical Layer (PHY) Specifications. Available at: http://standards.ieee.org/getieee802/download/802.11-2007.pdf.

[11] IEEE Computer Society. Local and metropolitan area networks - Specific requirements Part 15.1: Wireless medium access control (MAC) and physical layer (PHY) specifications for wireless personal area networks (WPANs). Available at: http://standards.ieee.org/getieee802/download/802.15.1-2005_part1.pdf.

[12] K. Jamieson and H. Balakrishnan. PPR: Partial Packet Recovery for Wireless Networks. In *SIGCOMM*, 2007.

[13] J. Jeong and C.-T. Ee. Forward Error Correction in Sensor Networks. In *WWSN*, 2007.

[14] S. Kim, R. Fonseca, and D. Culler. Reliable Transfer on Wireless Sensor Networks. In *SECON*, 2004.

[15] J. Ko, T. Gao, and A. Terzis. Empirical Study of a Medical Sensor Application in an Urban Emergency Department. In *BodyNets*, 2009.

[16] C.-J. M. Liang, J. Liu, L. Luo, A. Terzis, and F. Zhao. RACNet: A High-Fidelity Data Center Sensing Network. In *SenSys*, 2009.

[17] Measurement Computing Corp. USB-2523: USB-Based 16 SE/8 DI Multifunction Measurement and Control Board. Available from: http://www.mccdaq.com/usb-data-acquisition/USB-2523.aspx, 2009.

[18] R. Musaloiu-E. and A. Terzis. Minimising the Effect of WiFi Interference in 802.15.4 Wireless Sensor Networks. *International Journal of Sensor Networks*, 3(1):43–54, 2007.

[19] Phil Karn. Reed-Solomon Coding/Decoding Package v1.0. Available at http://www.piclist.com/tecHREF/method/error/rs-gp-pk-uoh-199609/index.htm., 1996.

[20] J. Polastre, R. Szewczyk, and D. Culler. Telos: Enabling Ultra-Low Power Wireless Research. In *IPSN/SPOTS*, 2005.

[21] S. Pollin, I. Tan, B. Hodge, C. Chun, and A. Bahai. Harmful Coexistence Between 802.15.4 and 802.11: A Measurement-based Study. In *CrownCom*, 2008.

[22] RF Micro Devices, Inc. ML2724 2.4 GHz Low-IF 1.5 MBps FSK Transceiver. Available from: http://www.rfmd.com/CS/Documents/ML2724_ML2724SPACEDatasheet.pdf, Dec. 2005.

[23] S. Y. Shin, H. S. Park, and W. H. Kwon. Mutual Interference Analysis of IEEE 802.15.4 and IEEE 802.11b. *Computer Networks*, 51(12):3338 – 3353, 2007.

[24] H. Soude, M. Agueh, and J. Mehat. Towards An optimal Reed Solomon Codes Selection for Sensor Networks: A Study Case Using TmoteSky. In *PE-WASUN*, 2009.

[25] K. Srinivasan, M. Kazandjieva, S. Agarwal, and P. Levis. The B-factor: Measuring Wireless Link Burstiness. In *SenSys*, 2008.

[26] Texas Instruments. 2.4 GHz IEEE 802.15.4 / ZigBee-ready RF Transceiver. Available at http://www.chipcon.com/files/CC2420_Data_Sheet_1_3.pdf, 2006.

[27] G. Thonet, P. Allard-Jacquin, and P. Colle. ZigBee - WiFi Coexistence: White Paper and Test Report. Technical report, Schneider Electrics, 2008.

[28] C. Won, J.-H. Youn, H. Ali, H. Sharif, and J. Deogun. Adaptive Radio Channel Allocation for Supporting Coexistence of 802.15.4 and 802.11b. In *VTC*, 2005.

[29] A. Woo and D. Culler. A Transmission Control Scheme for Media Access in Sensor Networks. In *MobiCom*, 2001.

[30] G. Zhou, Y. Wu, T. Yan, T. He, C. Huang, J. A. Stankovic, and T. F. Abdelzaher. A multi-frequency mac specially designed for wireless sensor network applications. *ACM Transactions in Embedded Computing Systems*, 9, 2010.